

# Platelet Kinetics in the Pulmonary Microcirculation in vivo Assessed by Intravital Microscopy

M.E. Eichhorn<sup>a</sup> L. Ney<sup>a,b</sup> S. Massberg<sup>c</sup> A.E. Goetz<sup>b</sup>

<sup>a</sup>Institute for Surgical Research, <sup>b</sup>Department of Anesthesiology, Klinikum Grosshadern, Ludwig Maximilians University, and <sup>c</sup>First Department of Internal Medicine, Klinikum Rechts der Isar, Technical University, Munich, Germany

## Key Words

Intravital microscopy · Lung · Microcirculation · Model · Platelet-endothelium interaction · Platelets · Thrombocytes

## Abstract

Growing evidence supports the substantial pathophysiological impact of platelets on the development of acute lung injury. Methods for studying these cellular mechanisms in vivo are not present yet. The aim of this study was to develop a model enabling the quantitative analysis of platelet kinetics and platelet-endothelium interaction within consecutive segments of the pulmonary microcirculation in vivo. New Zealand White rabbits were anesthetized and ventilated. Autologous platelets were separated from blood and labeled ex vivo with rhodamine 6G. After implantation of a thoracic window, microhemodynamics and kinetics of platelets were investi-

gated by intravital microscopy. Velocities of red blood cells (RBCs) and platelets were measured in arterioles, capillaries and venules, and the number of platelets adhering to the microvascular endothelium was counted. Kinetics of unstimulated platelets was compared with kinetics of thrombin-activated platelets. Velocity of unstimulated platelets was comparable to RBC velocity in all vessel segments. Unstimulated platelets passed the pulmonary microcirculation without substantial platelet-endothelial interaction. In contrast, velocity of activated platelets was decreased in all vascular segments indicating platelet margination and temporal platelet-endothelium interaction. Thrombin-activated platelets adhered to arteriolar endothelium; in capillaries and venules adherence of platelets was increased 8-fold and 13-fold, respectively. In conclusion, using intravital microscopy platelet kinetics were directly analyzed in the pulmonary microcirculation in vivo for the first time. In contrast to leukocytes, no substantial platelet-endothelium interaction occurs in the pulmonary microcirculation without any further stimulus. In response to platelet activation, molecular mechanisms enable adhesion of platelets in arterioles and venules as well as retention of platelets within capillaries.

The authors wish to dedicate this paper to Prof. Dr. med. Dr. h.c. mult. Konrad Messmer on the occasion of his 65th birthday.

Copyright © 2002 S. Karger AG, Basel

## KARGER

Fax +41 61 306 12 34  
E-Mail [karger@karger.ch](mailto:karger@karger.ch)  
[www.karger.com](http://www.karger.com)

© 2002 S. Karger AG, Basel  
1018-1172/02/0394-0330\$18.50/0

Accessible online at:  
[www.karger.com/journals/jvr](http://www.karger.com/journals/jvr)

Dr. med. Alwin E. Goetz  
Department of Anesthesiology, Klinikum Grosshadern  
Ludwig Maximilians University Munich, Marchioninistrasse 15  
D-81377 Munich (Germany)  
Tel. +49 89 7097 1844, Fax +49 89 7097 1848, E-Mail [agoetz@ana.med.uni-muenchen.de](mailto:agoetz@ana.med.uni-muenchen.de)

## Introduction

Platelets contribute to the maintenance of the intact circulation by preservation of vascular integrity and the control of hemorrhage after injury. However, under pathophysiologic conditions, platelets, similar to leukocytes, support inflammatory reactions by a wide range of mechanisms. Hence, platelets are known to play an important role in the pathogenesis of the acute respiratory distress syndrome [1] and postischemic reperfusion injury following lung transplantation [2].

Although platelets are anucleated cytoplasmic fragments of megakaryocytes, they possess a cellular machinery which is in many aspects comparable to that of leukocytes: platelets have a cytoskeleton facilitating cell motion. After activation, they produce oxygen radicals and release proinflammatory and vasoactive mediators such as thromboxane A<sub>2</sub>, leukotrienes, serotonin, platelet factor 4, and platelet-derived growth factor [1, 3, 4]. Furthermore, experimental evidence suggests that platelets may assist neutrophils in damaging the pulmonary vascular bed. First, histological studies of alveolar capillaries demonstrate that platelets are entrapped in the lung prior to an influx of neutrophils in an area of lung injury [5]. Second, neutrophil properties, such as chemotaxis, adherence and phagocytosis, are promoted by platelet release products. Finally, the combined bioconversion of metabolites of arachidonic acid between platelets, neutrophils and endothelial cells might significantly aggravate endothelial cell damage and contribute to further leukocyte activation and recruitment at the site of injury [6–9].

These mechanisms depend on platelet-endothelial and platelet-leukocyte interactions within the pulmonary microvascular bed mediated by a variety of adhesion molecules. However, *in vivo* no experimental data are available that delineate the nature of platelet dynamics and platelet-endothelial cell interactions within the pulmonary microcirculation – neither under physiologic conditions nor after platelet activation.

The aim of the present study, therefore, was to develop an *in vivo* model enabling the visualization and quantification of platelet kinetics and platelet-endothelial cell interactions in pulmonary arterioles, capillaries and venules and to determine whether platelet interactions with the microvascular endothelium are altered following platelet activation.

## Material and Methods

### *Animals*

Eleven adult male New Zealand White rabbits (Charles River, Sulzfeld, Germany) weighing 2.7–3.1 kg were used. All experimental procedures performed on rabbits were approved by the German legislation on the protection of animals. All animals received care in accordance with the 'Principles of Laboratory Animal Care' formulated by the National Society for Medical Research.

### *Surgical Procedure*

The animals were anesthetized by thiopental sodium (50 mg, *i.v.*), followed by  $\alpha$ -chloralose (50 mg/kg body weight, *i.v.*). For analgesia and neuromuscular blockade piritramide (0.5 mg/kg, *i.v.*) and pancuronium bromide (0.3 mg/kg, *i.v.*) were administered. After tracheotomy and intubation, the animals were ventilated mechanically at an inspiratory O<sub>2</sub> fraction of 0.4 and an inspiratory airway pressure of 9 mm Hg. To minimize atelectasis, end expiratory airway pressure was set to 2 mm Hg. Ventilation rate was 25/min with an inspiratory/expiratory ratio of 1:2. The animals received continuous infusion of normal saline (2 ml·h<sup>-1</sup>·kg<sup>-1</sup>, *i.v.*) to replace fluid loss by the lungs during ventilation and fluid loss by blood sampling. Rectal temperature was continuously measured and the body temperature of the animals was kept at 37.0 ± 0.5 °C by a feedback-controlled heating pad (Effenberger, Munich, Germany). Catheters were inserted into the aorta and superior vena cava through the carotid artery and jugular vein for recording of mean arterial and central venous pressure, blood sampling and injection of fluorescent erythrocytes and platelets, respectively. Cardiac output was measured by transpulmonary thermodilution (Ref-1, Baxter, Unterschleissheim, Germany) using a 5-french thermistor probe (Thermistor, Arrow, Erding, Germany) advanced into the abdominal aorta through the left femoral artery. Another catheter was inserted into the pulmonary artery to measure pulmonary artery pressure via a small thoracotomy in the left second intercostal space. The left thorax was closed and the rabbit was turned into the left lateral position for implantation of a transparent window into the right thoracic wall, as previously described in detail [10]. To prevent the exposed lung surface from drying or cooling, the window was superfused with gas-equilibrated Tyrode buffer warmed to 37 °C.

### *Cell Labeling and Intravital Microscopy*

Microvascular blood flow in subpleural arterioles, venules and alveolar capillaries was visualized by intravital microscopy after intravenous injection of fluorescein isothiocyanate (FITC)-labeled autologous red blood cells [10] (Sigma, Deisenhofen, Germany). Platelets were prepared according to Massberg et al. [11, 12]: 10 ml of whole blood was withdrawn from the carotid artery of the animal and collected in 15-ml polypropylene tubes containing 3 ml phosphate-buffered saline (PBS; Seromed, Berlin, Germany) and 0.55 ml aqua ad injectabilia containing 15.2 μmol citric acid, 30 μmol trisodium citrate, 40 μmol dextrose and 3 μg PGE<sub>1</sub>. The blood was centrifuged at 250 g for 10 min and platelet-rich plasma was gently transferred to a fresh tube containing identical chemicals as the first tube. The fluorescent dye rhodamine 6G (0.05%; 15 μl/ml platelet-rich plasma) was added and centrifugation was repeated at 2,000 g for 10 min. The sedimented pellet of platelets was resuspended in 2 ml of PBS. This resuspension contained approximately 10<sup>9</sup> platelets. The solution was injected intravenously shortly before intravital microscopy was performed. The purity of the cellular content of the platelet suspen-

sion was confirmed before infusion using a Coulter ACT Counter (Coulter, Miami, Fla., USA).

For intravital microscopic investigations, we used a modified Leitz Orthoplan microscope (Leitz, Wetzlar, Germany) with a 75 W XBO xenon lamp fitted with a  $\times 25$ , 0.6 numeric aperture, water immersion objective (Leitz). Selective visualization of FITC-labeled erythrocytes and rhodamine-6G-stained platelets was enabled using a Ploemopak illuminator (Leitz) with changeable filter blocks (Leitz L2 filter for FITC: excitation 450–490 nm, emission:  $525 \pm 20$  nm; Leitz N2 filter block for rhodamine 6G: excitation 530–560 nm, emission  $>580$  nm). Microscopic images were recorded by a silicon-intensified high-resolution (500 TV lines horizontal center resolution) target camera (C2400-08, Hamamatsu, Herrsching, Germany) and transferred to a video system (AG-7350, Panasonic, Munich, Germany). The magnification to the camera front was 312.5-fold, the resolution of the video microscope system on the monitor (PVM-2042QM, Sony, Munich, Germany) was approximately  $0.76 \times 0.56 \mu\text{m}$ . To exclude respiratory movements of the lung surface, microhemodynamics and platelet kinetics were observed during inspiratory plateau periods of 5 s.

#### Offline Video Analysis

Microhemodynamics and platelet kinetics were quantified in pulmonary arterioles and venules with diameters ranging from 21 to 41  $\mu\text{m}$ , and in capillary networks of subpleural alveolar areas. In each animal, one or two arterioles, two venules and two capillary networks were investigated.

Quantitative assessment of microhemodynamics and platelet kinetics was performed offline by frame-to-frame analysis using a digital image processing system (Optimas 3.0, Bioscan, Edmonds, Wash., USA.). Diameters of subpleural arterioles and venules, length of vessel segments and the mean velocity of labeled red blood cells ( $v_{\text{RBC}}$ ) passing a predefined vessel cross section were measured as described previously [10]. The flux of fluorescent platelets ( $f_{\text{PLT}}$ ) and red blood cells ( $f_{\text{RBC}}$ ) in arterioles and venules was quantified by counting the number of fluorescent cells passing the predefined vessel cross section and is given as number of fluorescent cells per second. Apparent wall shear rate ( $\gamma$ ) was calculated by Poiseuille's law for a Newtonian fluid:

$$\gamma = (v_b/D) 8.$$

Blood flow velocity ( $v_b$ ) was derived from  $v_{\text{RBC}}$  by correction for the Fahreus effect: the ratio of tube hematocrit ( $\text{Hct}_t$ ) and discharge hematocrit ( $\text{Hct}_d$ ) equals the ratio  $v_b/v_{\text{RBC}}$  [13].  $\text{Hct}_d$  was assumed to correspond to the systemic hematocrit as measured in blood drawn from the aorta and  $v_b$  was calculated using the following equation:

$$v_b = [\text{Hct}_d + (1 + \text{Hct}_d)(1 + 1.7e^{-0.415D} - 0.6e^{-0.011D})] v_{\text{RBC}}.$$

Platelets were classified according to their interaction with the endothelial cell lining as flowing and adherent cells. The velocity of each flowing platelet crossing a predefined cross section of each vessel was measured as the distance in axial direction of the vessel each platelet passed per unit of time. Mean platelet velocity ( $v_{\text{PLT}}$ ) was calculated as the harmonic mean of  $\geq 30$  single platelets. Adherent platelets were defined as cells not moving during the whole observation period of 5 s and are given as number of platelets per vessel wall area. A circular cross section of the vessels was assumed to calculate vessel wall area.

To determine the kinetics of erythrocytes and platelets in capillaries, the subpleural wall of a single alveolus was investigated during

three inspiration periods. The area of the alveolar wall was determined using the image-processing system. To determine the mean RBC velocity in the capillary network, the velocity of each labeled RBC crossing the boundary and entering the network was measured. For this purpose the pathways of FITC-labeled erythrocytes through the alveoli were marked on the screen of the computer, and RBC velocity was calculated by division of capillary length by alveolar transit time. Analogous to RBC velocity, the velocity of platelets in the capillary networks was measured. The number of platelets retained in the capillary network was counted and related to the alveolar surface area. Platelets were defined as retained, when they did not move for the whole 5-second observation period.

#### Experimental Protocol

The animals were placed on a table under the microscope and allowed to stabilize for 15 min after surgical preparation was completed. They were included in the study, if mean arterial pressure was greater than 75 mm Hg, oxygenation index ( $\text{PaO}_2/\text{FiO}_2$ ) exceeded 300 mm Hg and macroscopic inspection of the lung surface showed no signs of hemorrhage or altered perfusion. Then blood for platelet preparation was withdrawn from the carotid artery. FITC-labeled erythrocytes were injected intravenously and allowed to recirculate over a period of 30 min. Rhodamine-6G-labeled platelets were injected, macrohemodynamic parameters were measured, blood samples were withdrawn and intravital microscopy was performed (baseline assessment). After baseline measurements were completed, animals were randomly assigned to one of two experimental groups: in group 1, the stability of quantified parameters was investigated. Therefore, after a period of 60 min another batch of labeled platelets was injected, macrohemodynamics recorded and microhemodynamics as well as platelet kinetics were observed again. To ensure that the same alveoli and blood vessels were recorded in the different phases, respective x-y coordinates of the computer-controlled table were registered and recalled later on. In experimental group 2, the effect of thrombin-induced platelet activation on platelet kinetics and platelet-endothelial interactions was investigated. For that purpose, isolated and fluorescent-labeled platelets ( $\sim 10^9$ ) were incubated in vitro with thrombin (10 U; Thrombin, Sigma) over a period of 15 min at 25 °C, injected and observed 60 min after baseline assessment in the same vessel segments and alveolar areas as before. A sample size of 7 animals/group was intended. Since an interim analysis of data after the completion of 8 experiments (4 in each group) indicated that it was extremely unlikely that we would find any changes in the results observed in group 1, we decided not to use any more animals in this group. Subsequently, another 3 animals were subjected to the protocol of group 2.

#### Statistical Analysis

Data analysis was performed with a statistical software package (SigmaStat for Windows; Jadel Scientific, Erkrath, Germany). The Wilcoxon signed rank test was used to estimate stochastic probability in intragroup comparisons. Correlation was assessed by Spearman's coefficient of correlation. Normally distributed data are given as means  $\pm$  SEM; all other data are given as medians (1st quartile/3rd quartile). p values less than 0.05 were considered significant.

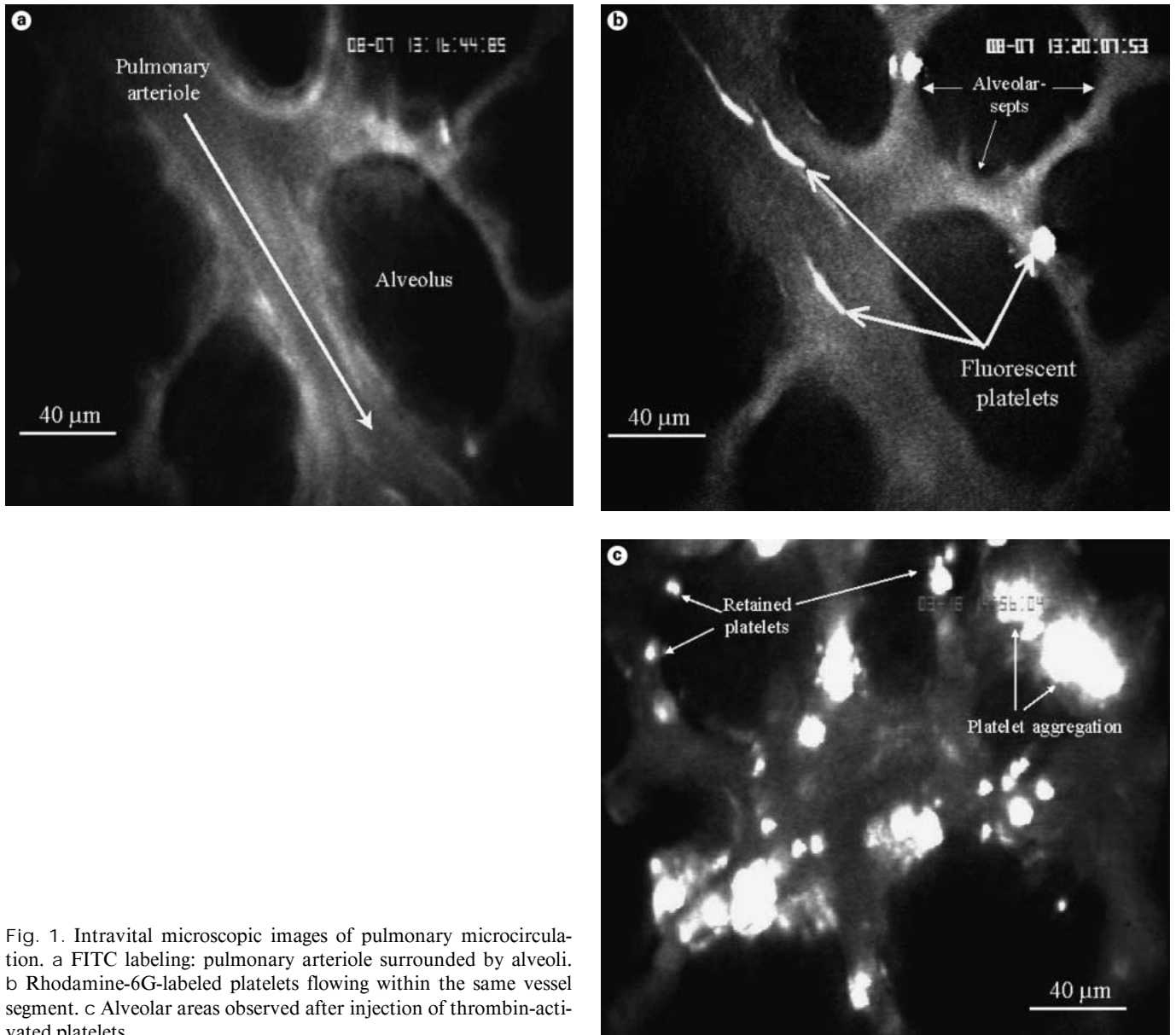


Fig. 1. Intravital microscopic images of pulmonary microcirculation. a FITC labeling: pulmonary arteriole surrounded by alveoli. b Rhodamine-6G-labeled platelets flowing within the same vessel segment. c Alveolar areas observed after injection of thrombin-activated platelets.

## Results

### *Platelet Preparation for Intravital Microscopy*

As ascertained before infusion by flow cytometry and by use of a Coulter ACT counter, platelet separation by differential centrifugation yielded a platelet suspension with negligible amounts of other cellular components. Less than 5 leukocytes/ $10^6$  platelets were found in the platelet preparations used for the present study. Platelets showed excellent fluorescent labeling, indicated by high fluorescent intensity measured by flow cytometry. Cyto-

logical evaluation showed a discoid shape and no platelet aggregates. Blood sampling and injection of labeled platelets had no effects on heart rate, arterial and pulmonary arterial blood pressure and arterial blood gases.

### *Macrohemodynamic, Microhemodynamics and Platelet Kinetics during Baseline Assessment*

There were no statistical differences in any parameter between the study groups at baseline measurements. Therefore, data of baseline measurements were pooled

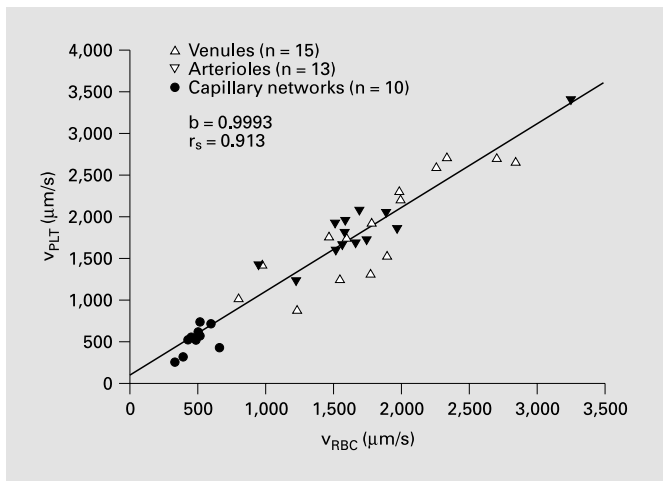


Fig. 2. Correlation between erythrocyte velocity ( $v_{RBC}$ ) and platelet velocity ( $v_{PLT}$ ) in arterioles, capillaries and venules observed in 11 animals at baseline.  $r_s$  = Spearman's coefficient of correlation;  $b$  = slope.

and are presented as mean of all animals ( $n = 11$ ) used in both groups. During baseline assessment of platelet kinetics, mean arterial pressure was  $87 \pm 2.9$  mm Hg, mean pulmonary artery pressure was  $16.4 \pm 0.8$  mm Hg, central venous pressure was  $4.8 \pm 0.7$  mm Hg, and cardiac output was  $251 \pm 10$  ml/min. Mean pulmonary artery pressure divided by cardiac output (PVR index) was calculated as the index of pulmonary vascular resistance. The PVR index was  $67 \pm 5$  mm Hg·min·l<sup>-1</sup>. Arterial oxygen tension, carbon dioxide tension and pH during baseline was  $159 \pm 13$  mm Hg,  $43 \pm 4$  mm Hg and  $7.35 \pm 0.02$ , respectively.

In 11 animals, 13 arterioles and 15 venules with diameters ranging from 23 to 32 and from 22 to 41  $\mu\text{m}$ , respectively (table 1), were analyzed and data included in the calculation of the median and quartiles. No firm adhesion of unstimulated platelets was observed in arterioles. Only few platelets adhering to the microvascular endothelium could be observed in venules. Shear rates in arterioles did not differ from shear rates in venules. The mean velocity of flowing platelets was close to the mean red blood cell velocity in arterioles as well as in venules, as indicated by a ratio of  $v_{PLT}/v_{RBC}$  close to 1.

In 11 alveoli with alveolar wall surface areas ranging from  $12 \cdot 10^3$  to  $33 \cdot 10^3$   $\mu\text{m}^2$ , microhemodynamics and platelet kinetics were investigated (table 2). As expected, in alveolar capillaries mean corpuscular velocities were significantly slower than in arterioles and venules, but there was no significant difference between  $v_{PLT}$  and  $v_{RBC}$

Table 1. Microhemodynamics and platelet kinetics in pulmonary arterioles and venules

Parameters	Arterioles	Venules
Diameter, $\mu\text{m}$	26.8 (25.8; 30.5)	27.4 (25.3; 28.7)
$v_{RBC}$ , $\mu\text{m/s}$	1,621 (1,548; 1,814)	1,648 (1,501; 2,132)
$f_{RBC}$ , cells/s	24.2 (17.7; 29.5)	25.0 (20.0; 33.0)
$\gamma$ , 1/s	270 (256; 297)	266 (257; 339)
$v_{PLT}$ , $\mu\text{m/s}$	1,866 (1,675; 1,958)	1,748 (1,126; 2,444)
$f_{PLT}$ , cells/s	7.7 (4.8; 13.2)	10.0 (8.1; 15.4)
$v_{PLT}/v_{RBC}$	1.06 (1.04; 1.21)	1.00 (0.90; 1.18)
$AD_{PLT}$ , cells/ $\text{mm}^2$	0 (0; 0)	0 (0; 0)

Values are given as medians (1st quartile; 3rd quartile).  $v_{RBC}$  = Mean erythrocyte velocity;  $f_{RBC}$  = red blood cell flux;  $\gamma$  = apparent shear rate;  $v_{PLT}$  = mean platelet velocity;  $f_{PLT}$  = platelet flux;  $AD_{PLT}$  = number of endothelium-adherent platelets related to vessel wall area. Values were quantified in 13 arterioles and 15 venules at baseline in 11 animals ( $n = 11$ ).

Table 2. Microhemodynamics and platelet kinetics in capillary networks

Parameters	Capillaries
Alveolar area, $10^3/\mu\text{m}^2$	18.9 (16.3; 22.9)
Capillary length, $\mu\text{m}$	1,083 (896; 1,296)
$v_{RBC}$ , $\mu\text{m/s}$	493 (435; 517)
$v_{PLT}$ , $\mu\text{m/s}$	536 (447; 606)
$v_{PLT}/v_{RBC}$	1.15 (0.87; 1.22)
Retained cells	10.8 (0; 38.3)

Values are given as medians (1st quartile; 3rd quartile) of 10 alveolar capillary networks investigated in 10 animals.  $v_{RBC}$  = Mean erythrocyte velocity;  $v_{PLT}$  = mean platelet velocity; retained cells = number of platelets retained for periods  $> 5$  s observed in the capillary network of alveoli.

in capillaries. Mean transit time of platelets to pass the alveolar capillary network was  $31.0 \pm 1.8$  ms. The majority of platelets passed the alveolar capillary network without being permanently retained within the capillaries. A significant correlation between  $v_{RBC}$  and  $v_{PLT}$  over all vascular segments, arterioles, capillaries and venules was found under baseline conditions (fig. 2).

#### Stability of Quantified Parameters

In experimental group 1, the stability of the observed parameters was assessed over a time period of 60 min in

Table 3. Stability of quantified parameters

Macrohemodynamics		Microhemodynamics		Platelet kinetics	
AP <sub>m</sub>	98.0 ± 6.6	v <sub>RBC</sub> art.	100.5 ± 8.1	v <sub>PLT</sub> art.	102.3 ± 13.9
PAP <sub>m</sub>	102.9 ± 11.2	v <sub>RBC</sub> cap.	96.7 ± 6.3	v <sub>PLT</sub> cap.	93.7 ± 6.3
CO	100.5 ± 7.6	v <sub>RBC</sub> ven.	110.3 ± 17.4	v <sub>PLT</sub> ven.	100.9 ± 28.1
		f <sub>RBC</sub> art.	97.1 ± 12.1	f <sub>PLT</sub> art.	115.2 ± 24.2
		f <sub>RBC</sub> ven.	109.0 ± 8.8	f <sub>PLT</sub> ven.	112.0 ± 12.2

Percent changes in macrohemodynamics, microhemodynamics and platelet kinetics 60 min after baseline assessment measured in 4 animals. Results are given as means ± SEM in % of baseline values. AP<sub>m</sub> = Mean arterial pressure; PAP<sub>m</sub> = mean pulmonary arterial pressure; CO = cardiac output; v<sub>RBC</sub> = mean erythrocyte velocity in arterioles (art., n = 6), capillary networks (cap., n = 4) and venules (ven., n=7); v<sub>PLT</sub> = mean platelet velocity in arterioles, capillaries and venules; f<sub>RBC</sub> = red blood cell flux; f<sub>PLT</sub> = platelet flux in arterioles and venules.

order to ascertain the validity of the model. In table 3, relative changes in macrohemodynamics, microhemodynamics and platelet kinetics are summarized. In none of the parameters, statistically significant changes occurred during the 60-min observation period.

#### *Impact of Platelet Activation on Platelet Kinetics*

In order to study the effect of activation of platelets on their kinetics and interaction with endothelial cells in pulmonary arterioles, capillaries and venules, in 7 animals (group 2) fluorescent platelets were activated with thrombin prior to injection and observed in identical vessels 60 min after baseline assessment.

Macrohemodynamic parameters, arterial blood gases and microhemodynamic parameters did not significantly change following injection of activated platelets. Arterial pressure was 91 ± 4 mm Hg, mean pulmonary arterial pressure 15 ± 1 mm Hg, central venous pressure 5 ± 1 mm Hg, cardiac output was 241 ± 6 ml/min and the PVR index 63 ± 4 mmHg·min·l<sup>-1</sup>. Arterial oxygen tension was 166 ± 13 mm Hg, carbon dioxide tension 46 ± 5 mm Hg and pH 7.34 ± 0.03. Median erythrocyte velocities in arterioles (1,676; 1,539–1,929 μm/s), capillaries (585; 429–603 μm/s) and venules (1,634; 1,535–2,141 μm/s) as well as red blood cell flux (23.1; 20.8–26.9 s<sup>-1</sup>) and apparent shear rates in arterioles (277; 257–311 s<sup>-1</sup>) and venules (f<sub>RBC</sub>: 25.2; 22.5–29.8 s<sup>-1</sup>; shear rate: 289; 248–289 s<sup>-1</sup>) remained constant compared with baseline values. In contrast to microhemodynamic parameters, significant changes in platelet dynamics and platelet-endothelium interactions occurred in response to platelet activation. The median platelet velocity was reduced by 24% in arterioles (1,419; 1,004–1,559 μm/s), by 19% in

capillaries (439; 330–548 μm/s), being significantly decreased by 34% in venules (1,150; 1,093–1,231 μm/s). Frequency distributions of single platelet velocities were established for pulmonary arterioles and venules (fig. 3). Injection of activated platelets induced a shift to the left of the velocity distribution in arterioles, resulting in the appearance of low-velocity (less than 500 μm/s) platelets indicating platelet margination within arterioles. In venules, skewness after injection of activated platelets decreased by 19%, resulting in a left shift of the distribution. The number of platelets flowing with a velocity below 500 μm/s was 7-fold increased after platelet activation. In comparison to baseline values, platelet flux was reduced by 34% (baseline: 8.3; 6.5–14.4 s<sup>-1</sup>; PLT<sub>act</sub>: 5.5; 2.2–10.1 s<sup>-1</sup>) in arterioles and by 48% (significant difference) in venules (baseline: 12.4 s<sup>-1</sup>; 8.9–19.0; PLT<sub>act</sub>: 6.5; 1.2–12.5 s<sup>-1</sup>).

Mean alveolar transit time of flowing platelets was prolonged from 30.4 ± 2.6 to 45.3 ± 9.7 ms without reaching a significant level. There still was a strong correlation between mean erythrocyte velocity and the velocity of activated platelets (fig. 4, Spearman's coefficient of correlation = 0.801). However, after platelet activation the slope of the line of regression was reduced by ~52%.

While no firmly adherent platelets could be observed in arterioles during baseline assessment, after platelet activation platelets adhered to arteriolar endothelium (49.1; 0–82 mm<sup>-2</sup>; fig. 5). Accordingly, there was a significant increase in endothelial-adherent platelets in response to platelet activation in venules. Also, in the alveolar capillaries the number of permanently retained platelets was elevated ~8-fold. Isolated platelet aggregates within the capillary networks could be observed (fig. 1c).

Fig. 3. Frequency distribution of platelet velocities in arterioles (a, b) and venules (c, d) after injection of unstimulated (a, c) and thrombin-activated platelets (b, d). a n = 252, skewness = 1.10. c n = 287, skewness = 1.39. b n = 193, skewness = 1.07. d n = 231, skewness = 1.12.

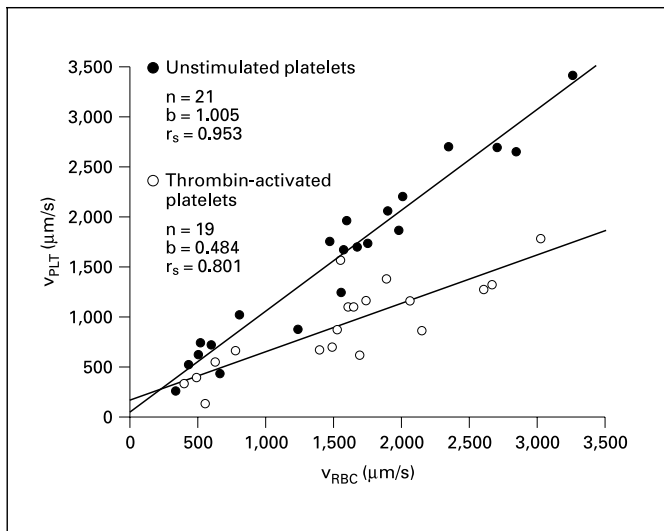
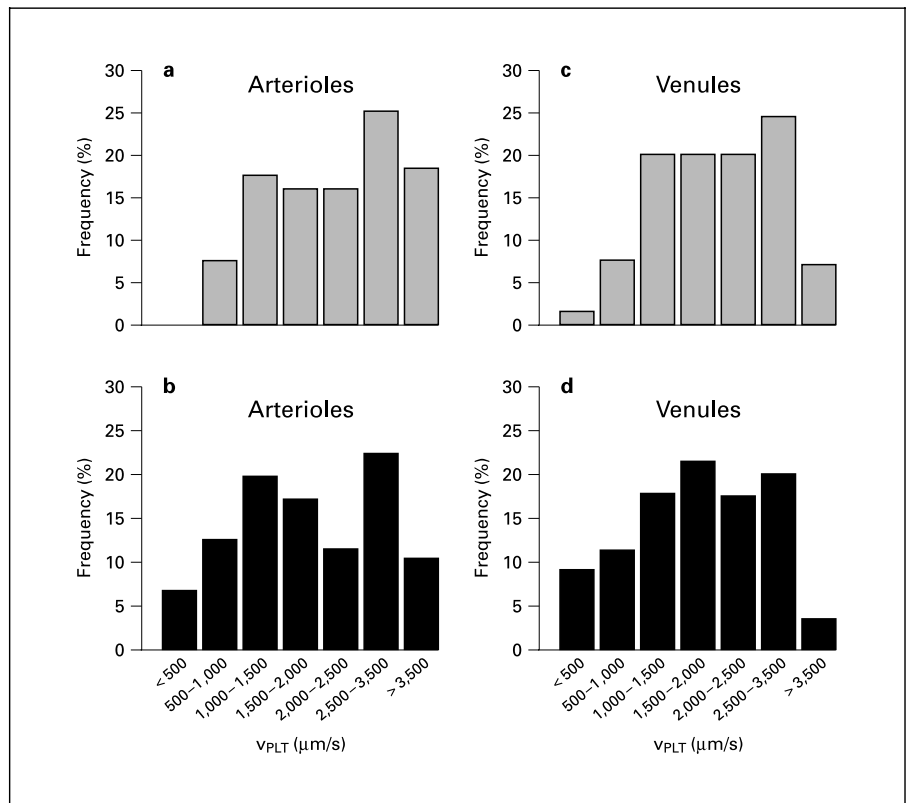


Fig. 4. Correlation between erythrocyte velocity ( $v_{RBC}$ ) and platelet velocity ( $v_{PLT}$ ) after injection of unstimulated and thrombin-activated platelets in arterioles, alveolar networks and venules in animals of group 2 (n = 7).  $r_s$  = Spearman's correlation coefficient.

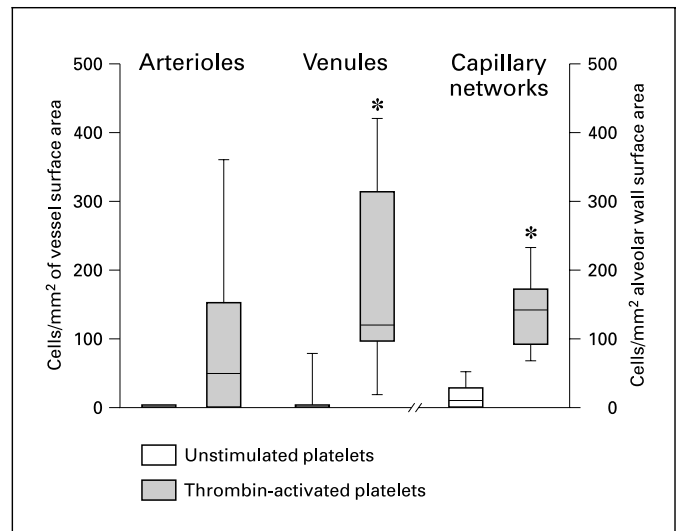


Fig. 5. Adherent platelets in arterioles (n = 7) and venules (n = 8) related to vessel surface area, and retained platelets in capillary networks (n = 6) related to alveolar wall surface area observed in 7 animals (n = 7). Values are given as medians, 1st to 3rd quartiles, and 5th and 95th percentiles. \*  $p < 0.05$ ,  $PLT$  vs.  $PLT_{act}$ , Wilcoxon signed rank test.

## Discussion

### *Model*

The model presented is the first one enabling simultaneous quantification of macrohemodynamics, microhemodynamics and platelet kinetics in pulmonary arterioles, alveolar capillaries and venules of the ventilated rabbit lung using intravital fluorescence microscopy in combination with ex vivo labeling of autologous thrombocytes. Detailed knowledge about platelet kinetics and platelet-endothelial interactions is of utmost importance as platelet sequestration, and platelet-endothelial and platelet-leukocyte interactions within the pulmonary microcirculation might represent decisive pathophysiological steps leading to the development of the acute respiratory distress syndrome and postischemic reperfusion injury following lung transplantation [2].

Recent studies on platelet kinetics within the pulmonary microcirculation used radioactive cell labeling techniques [14] or morphometric analysis based on lung transmission electron micrographs [15]. Both techniques do not enable direct visualization and quantitative assessment of platelet kinetics in all segments of the pulmonary microcirculation in vivo. Either resolution is not able to clarify the local site and quantity of platelet-endothelial interactions or only static postmortem investigations are performed. Although intravital microscopy combined with the transthoracic window technique had already been described in 1939 by Terry et al. [16], this method has not yet been used to investigate platelet kinetics in the pulmonary microcirculation.

Since no fluorescent dye may exclusively stain platelets after in vivo injection, we have chosen an ex vivo labeling technique for platelets with rhodamine 6G for two reasons: First, when fluorescent dyes (rhodamine 6G, acridine orange), which are routinely used for cellular staining in intravital microscopic studies, are injected in the systemic circulation, they predominantly stain leukocytes. In this case, the brightness of leukocytes would far exceed the less fluorescent intensity of platelets. This is of particular relevance in the pulmonary microcirculation where a large amount of leukocytes is marginated under physiologic conditions. Second, in vivo injection of any dye would stain all circulating platelets. Considering the platelet count, this would inhibit identification of individual cells and therefore compromise quantification of platelet velocities and interaction with the pulmonary endothelium. The staining method used in this study has been proven to be valid and useful for investigations of platelet kinetics and mechanisms of platelet-endothelial interac-

tions in the mouse small intestine following ischemia-reperfusion [11, 12].

### *Microhemodynamics and Platelet Kinetics in Pulmonary Arterioles, Capillaries and Venules*

The  $v_{RBCs}$  values quantified in pulmonary arterioles and venules are higher than those obtained in a recent study [17], in which vessels with larger diameters than in the present investigation were investigated.  $v_{RBC}$  values in alveolar capillaries were comparable to those measured in recent studies.

In the literature, experimental data on platelet velocities in the pulmonary microcirculation have not been published so far. In the present study,  $v_{PLT}$  of unstimulated platelets did not show significant differences compared to mean red blood cell velocities, neither in arterioles nor in capillaries or venules. A strong correlation between erythrocyte and platelet velocities in all vascular segments was observed. These results indicate that the velocity profiles of platelets and red blood cells within the pulmonary microcirculation might be similar under physiologic conditions. However, we cannot rule out that differences in the distribution over the cross sectional area and the velocity profile might actually cancel each other out. Comparing velocities at the same relative radial distribution, Tangelder et al. [18] demonstrated that the shapes of the velocity profiles of platelets and red blood cells are similar in mesentery arterioles (diameter: 17–32  $\mu\text{m}$ ) of the rabbit. Woldhuis et al. [19] observed that concentration profiles of blood platelets differ in arterioles and venules. They demonstrated in vivo that near the vessel wall the number of platelets per unit volume is significantly higher in arterioles compared with venules. In contrast, in venules the mean platelet density is higher in the center of the vessel. Assuming a parabolic profile of velocity within a microvessel, one could expect a lower mean platelet velocity in arterioles than in venules. We were not able to confirm this phenomenon in our model as mean platelet velocities in arterioles and venules were not significantly different.

Using radiolabeled platelets, Doerschuk et al. [14] investigated the behavior of platelets during their passage through the pulmonary circulation after central venous injection by means of  $\gamma$  scintillation technique. The fraction of injected cells remaining in the lung was approximately 3% after 10 min of circulation, indicating that there is no substantial pool of platelets retained in the lung. In accordance with these data, we were not able to observe substantial margination of unstimulated platelets within the pulmonary microvascular bed. During baseline



investigation, we did not observe platelet adhesion to the arteriolar endothelium at all, whereas a small number of platelets were retained within capillaries or adhered to venular endothelium. In view of this finding, platelets exhibit a completely different behavior in comparison to leukocytes. It is well known that under physiological conditions the marginated pool of leukocytes sequestered in the pulmonary microcirculation exceeds the total number of circulating leukocytes two- to threefold [20]. There might also be several mechanisms enabling interaction between platelets and marginated leukocytes. However, at least platelets without additional stimulation seem to pass the microvascular bed without any substantial interaction with endothelial cells or leukocytes, similar to red blood cells.

#### *Impact of Platelet Activation by Thrombin on Platelet Kinetics*

Thrombin is a multifunctional protease generated at sites of vascular injury and is known to be a potent agonist that elicits in platelets physiological responses such as shape changes, aggregation and granular content secretion [21]. The cellular transduction of thrombin activity includes the activation of thrombin-receptor-associated GTP-binding proteins and the subsequent stimulation of phospholipase C and phospholipase A<sub>2</sub> [22]. Activation of phospholipase C results in hydrolysis of inositol phospholipids, i.e. phosphatidylinositol 4,5-bisphosphate. This hydrolysis causes the formation of 1,2-diacylglycerol and inositol 1,4,5-triphosphate resulting in rapid mobilization of Ca<sup>2+</sup> from the platelet-dense tubular system to the cytosol. Consequently,  $\alpha$  granule membranes fuse with plasma membrane, and  $\alpha$  granule proteins as well as several coagulation factors (fibrinogen, von Willebrand factor, factor V or fibronectin) are released. When the internal surface of  $\alpha$  granules is exteriorized, the lectin-like adhesion molecule GMP140 (CD 62) is rapidly mobilized to the cell surface as an integral membrane protein enabling platelet-leukocyte and platelet-endothelial interactions independent of de novo synthesis of mRNA or proteins [23]. In addition, platelet activation by thrombin causes a structural change in platelet membrane integrins such as the GPIIb-IIIa (CD41/CD62) receptor that causes exposure of fibrinogen binding sites. Hence, the structural changes in the receptor enable platelets to bind to soluble fibrinogen, fibronectin or von Willebrand factor and thus platelet-platelet aggregation [23].

We observed a decreased mean platelet velocity, enhanced platelet-endothelial interaction and platelet aggregation within the pulmonary microvascular bed after

infusion of thrombin-activated platelets. The decreased mean platelet velocity in arterioles and venules is mainly caused by a shift to the left of the velocity distribution. These slow velocities might be due to temporal interactions of platelets with the endothelium (rolling, temporal adhesion). Macrohemodynamics, microhemodynamics and calculated apparent shear rates did not change following injection of activated platelets. Shear-dependent mechanisms as a possible cause of enhanced platelet-endothelial interactions may therefore be ruled out. Mechanisms depending on adhesion molecules [mainly structural (GP IIB/IIIa, GP I-IX) and quantitative changes (CD 62) of platelet adhesion molecules] seem to be responsible for enhanced platelet-endothelial interactions, as platelets were incubated in vitro with thrombin and hence pulmonary microvascular endothelium was not subjected to additional proaggregatory activation.

In the lung, platelet-endothelium interaction after platelet activation was more pronounced in venules than in arterioles. Red blood cell velocities and apparent shear rates were not different between arterioles and venules, and therefore the most conclusive explanation for this finding might be a difference in the endothelial surface properties, e.g. the glycocalyx composition of the microvascular endothelium. Perry and Granger [24], for example, noted a lower density of adhesion receptors on arteriolar than on venular endothelium in 25- to 35- $\mu$ m cat mesenteric vessels. However, in this context the above-mentioned marginated pool of leukocytes within the pulmonary microcirculation has to be discussed, too. Comparing arterioles and venules with diameters ranging from 14 to 33 and from 11 to 29  $\mu$ m, respectively, Kuebler et al. [17] have demonstrated that the number of endothelial adherent leukocytes in venules exceeds the number of adherent leukocytes in arterioles approximately 3.5-fold. Especially for venules, it is well conceivable that also enhanced platelet-leukocyte interactions mediated for example by P-selectin may first slow down the velocity of activated platelets and therefore contribute to platelet margination and further platelet adhesion to the venular endothelium.

The largest amount of activated platelets is retained in the capillary networks of lung alveoli, above all as the accumulated vascular surface of the capillaries far exceeds the vascular surface of pulmonary arterioles and venules. However, the mechanisms responsible for platelet accumulation within the pulmonary capillary network are yet unknown. While leukocyte retention in alveolar capillaries probably results from mechanical hindrance of leukocyte transit through narrow capillary segments [25] and,

in addition, by fucoidin-sensitive interactions of leukocytes with the capillary endothelium [26], these mechanisms cannot be completely translated to platelets. Because platelets are small, discoid cytoplasmic fragments with diameters of 2–3  $\mu\text{m}$  and the mean capillary diameter can be assumed to be 5.78  $\mu\text{m}$  [27], a mechanical hindrance of platelet transit through the capillary segments is unlikely to be the main reason for platelet sequestration. Therefore one could assume operational mechanisms mediated by adhesion molecules responsible for the accumulation of activated platelets within the capillary networks.

In conclusion, our present study has shown that *ex vivo* labeling and recirculation of autologous platelets enable to investigate platelet dynamics within the consecutive segments of the pulmonary microcirculation by means of

intravital fluorescence microscopy. After thoracic window implantation, the preparation remained stable and thus is useful for measurements of platelet kinetics in the same microvessel under different experimental conditions. For the first time velocities of unstimulated platelets within pulmonary arterioles, capillaries and venules were quantified. In contrast to leukocytes, no substantial platelet-endothelium interaction within the pulmonary microcirculation was observed under physiological conditions. However, after activation platelet-endothelium interactions occur in all segments of the pulmonary microcirculation. Further studies are needed to elucidate the molecular mechanisms and pathophysiologic consequences of platelet-endothelium and platelet-leukocyte interactions in view of the development of acute lung injury.

## References

- Heffner JE, Sahn SA, Repine JE: The role of platelets in the adult respiratory distress syndrome. Culprits or bystanders? *Am Rev Respir Dis* 1987;135:482–492.
- Okada Y, Marchevsky AM, Zuo XJ, et al: Accumulation of platelets in rat syngeneic lung transplants: A potential factor responsible for preservation-reperfusion injury. *Transplantation* 1997;64:801–806.
- Piccardoni P, Evangelista V, Piccoli A, de Gaetano G, Walz A, Cerletti C: Thrombin-activated human platelets release two NAP-2 variants that stimulate polymorphonuclear leukocytes. *Thromb Haemost* 1996;76:780–785.
- Deuel TF, Senior RM, Chang D, Griffin GL, Heinrikson RL, Kaiser ET: Platelet factor 4 is chemotactic for neutrophils and monocytes. *Proc Natl Acad Sci USA* 1981;78:4584–4587.
- Barry BE, Crapo JD: Patterns of accumulation of platelets and neutrophils in rat lungs during exposure to 100% and 85% oxygen. *Am Rev Respir Dis* 1985;132:548–555.
- Barry OP, Pratico D, Lawson JA, FitzGerald GA: Transcellular activation of platelets and endothelial cells by bioactive lipids in platelet microparticles. *J Clin Invest* 1997;99:2118–2127.
- Evangelista V, Celardo A, Dell'Elba G, et al: Platelet contribution to leukotriene production in inflammation: In vivo evidence in the rabbit. *Thromb Haemost* 1999;81:442–448.
- Pfister SL, Deinhard DD, Campbell WB: Methacholine-induced contraction of rabbit pulmonary artery: Role of platelet-endothelial transcellular thromboxane synthesis. *Hypertension* 1998;31:206–212.
- Lou J, Donati YR, Juillard P, et al: Platelets play an important role in TNF-induced microvascular endothelial cell pathology. *Am J Pathol* 1997;151:1397–1405.
- Kuhnle GE, Leipfinger FH, Goetz AE: Measurement of microhemodynamics in the ventilated rabbit lung by intravital fluorescence microscopy. *J Appl Physiol* 1993;74:1462–1471.
- Massberg S, Eisenmenger S, Enders G, Krombach F, Messmer K: Quantitative analysis of small intestinal microcirculation in the mouse. *Res Exp Med (Berl)* 1998;198:23–35.
- Massberg S, Enders G, Leiderer R, et al: Platelet-endothelial cell interactions during ischemia/reperfusion: The role of P-selectin. *Blood* 1998;92:507–515.
- Pries AR, Secomb TW, Gaetgens P, Gross JP: Blood flow in microvascular networks – Experimental and simulation. *Circ Res* 1990;67:826–834.
- Doerschuk CM, Downey GP, Doherty DE, et al: Leukocyte and platelet margination within microvasculature of rabbit lungs. *J Appl Physiol* 1990;68:1956–1961.
- Helset E, Lindal S, Olsen R, Myklebust R, Jorgensen L: Endothelin-1 causes sequential trapping of platelets and neutrophils in pulmonary microcirculation in rats. *Am J Physiol* 1996;271:L538–L546.
- Terry RJ: A thoracic window for observation of the lung in a living animal. *Science* 1939;90:43–44.
- Kuebler WM, Kuhnle GE, Groh J, Goetz AE: Leukocyte kinetics in pulmonary microcirculation: Intravital fluorescence microscopic study. *J Appl Physiol* 1994;76:65–71.
- Tangelder GJ, Slaaf DW, Muijtens AM, Arts T, oude Egbrink MG, Reneman RS: Velocity profiles of blood platelets and red blood cells flowing in arterioles of the rabbit mesentery. *Circ Res* 1986;59:505–514.
- Woldhuis B, Tangelder GJ, Slaaf DW, Reneman RS: Concentration profile of blood platelets differs in arterioles and venules. *Am J Physiol* 1992;262:H1217–H1223.
- Doerschuk CM, Allard MF, Martin BA, MacKenzie A, Autor AP, Hogg JC: Marginated pool of neutrophils in rabbit lungs. *J Appl Physiol* 1987;63:1806–1815.
- Blockmans D, Deckmyn H, Vermeylen J: Platelet activation. *Blood Rev* 1995;9:143–156.
- Lapetina EG: The signal transduction induced by thrombin in human platelets. *FEBS Lett* 1990;268:400–404.
- Body SC: Platelet activation and interactions with the microvasculature. *J Cardiovasc Pharmacol* 1996;27(suppl 1):S13–S25.
- Perry MA, Granger DN: Role of CD11/CD18 in shear rate-dependent leukocyte-endothelial cell interactions in cat mesenteric venules. *J Clin Invest* 1991;87:1798–1804.
- Doerschuk CM: Mechanisms of leukocyte sequestration in inflamed lungs. *Microcirculation* 2001;8:71–88.
- Kuebler WM, Kuhnle GE, Groh J, Goetz AE: Contribution of selectins to leukocyte sequestration in pulmonary microvessels by intravital microscopy in rabbits. *J Physiol (Lond)* 1997;501:375–386.
- Guntheroth WG, Luchtel DL, Kawabori I: Pulmonary microcirculation: Tubules rather than sheet and post. *J Appl Physiol* 1982;53:510–515.